In the wake of the wind: Can wind turbine parameterizations in WRF improve estimates of power production by future offshore wind farms in California?

D.J. Rasmussen *

Department of Civil and Environmental Engineering, University of California, Davis

ABSTRACT

In order to meet an aggressive renewable energy portfolio standard, California may make a move towards offshore wind generated electricity over the next decade. A previous study has shown that the Cape Mendocino region of California has both ideal wind resources and coastal bathymetry to accommodate the current generation of wind turbine technology. This proposed wind farm is anticipated to supply an average of 790 MW of gross renewable power. However, this estimate assumes an homogenous distribution of wind resources across all offshore wind turbines. Observational studies have shown that wind turbine wake effects can lead to appreciable downstream losses of wind resources through the production of turbulent kinetic energy (TKE). A numerical modeling exercise is performed using the Advanced Weather and Research Forecasting model (ARW) with wind turbine parameterizations that physically represent a wind turbine as a sink for momentum and a source for TKE. Results show a decrease in 100 m wind speeds of up to 3 m s^{-1} and a 40% reduction in power production within the proposed Cape Mendocino large offshore wind turbine array. These results suggest that prior estimates of future wind generated electricity may be greatly over predicted if wind turbine wake effects are not included in the calculations.

1. Introduction

Wind turbines make use of the kinetic energy in the wind to generate electricity. In addition to renewable power generation, wind turbines produce turbulence in their wake, much like a ship propelling itself through water. These turbulent effects are often not significant for most local-scale commercial wind farms, which typically have only 1 or 2 rows of wind turbines spaced 5–10 rotor diameters apart. However, as interest in the development of large offshore wind turbine arrays expands to meet existing renewable portfolio standards (e.g. CA Senate Bill X1-2 (2011)), the importance of investigating the effects of wind turbine wake on downstream power production grows.

In a study assessing observed wake effects at large wind farms, Christiansen and Hasager (2005) used satellite synthetic aperture radar (SAR) and calculated an average reduction in 10 m wind speeds of 8–9% (0.5–1.5 m s^{-1}) immediately downstream of both the Horns Rev (80 turbines) and the Nysted (78 turbines) offshore wind farms in Denmark. The wind speeds recover to roughly 98% of their initial velocities over a distance of 5–20 km downstream of the wind farms. More recently, Smalikho et al. (in press) used coherent Doppler lidar to measure the wake produced by one turbine at the National Renewable Energy Lab (NREL). They found a wind velocity deficit behind the turbine of 27% to 74% with the wake extending from 120 m up to 1180 m. Their results were dependent on the ambient atmospheric stability and the wind speed at the turbine hub-height.

Many studies estimating the total global wind energy power production potential assume local-scale conditions whereby wake effects are assumed negligible and all turbines over large regions produce equivalent power from equivalent wind resources (Archer and Jacobson 2005; Jacobson and Archer 2012; Lu et al. 2009); these studies are likely over estimating the total wind power production potential (Adams and Keith 2013).

a. The propsed Cape Mendocino offshore wind farm

A recent study proposes that the Cape Mendocino area of California has sufficient wind resources during the day and night throughout the year to supply roughly 790 megawatts (MW) of electricity to both the city of Eureka and the greater Humboldt County region (Dvorak et al. 2010). They conclude wind resources are greatest during the month of July. Additionally, the Cape Mendocino coastal region is characterized by bathymetry that is accommdating to the current generation of wind turbine foundation technology ($\leq$ 50 m). Figure 1 shows the extent of the proposed wind farm and the local coastal bathymetry.

Using roughly 300 REpower 5.0 MW turbines, the pro-

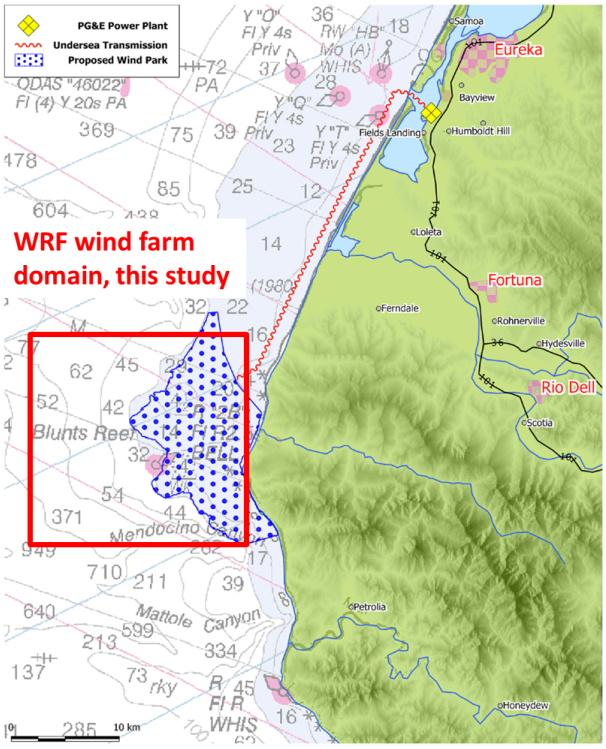

FIG. 1. A map showing the location of a proposed offshore wind farm at Cape Mendocino. Coastal bathymetry (meters) is contoured in gray. An undersea power transmission cable is shown as a red squiggly line. The red rectangle corresponds to the wind farm parameterized in the WRF model in this study (section 3.). Figure from Dvorak et al. (2010).

posed wind farm at Cape Mendocino would cover 138 km^2 of ocean surface. Dvorak et al. (2010) perform a simple calculation of the proposed wind farm's average power production assuming no wake effects and conclude that, on averge, roughly 790 MW of electricity could be generated by the farm.

2. WRF wind turbine parameterizations

Fitch et al. (2012) develop a wind farm parameterization for the Weather Research and Forecasting (WRF) model to investigate the effects of a wind farm on the surrounding atmosphere. The Fitch et al. wind farm parameterizations act as a sink for momentum within the PBL that converts the KE of the mean flow to both turbulent kinetic energy (TKE) and power. Previous studies have used increased surface roughness to parameterize wind farms in numerical models (Barrie and Kirk-Davidoff 2010). This approach is likely too simplistic as it neglects the known production of turbulence and wind shear generated by the wind turbines.

Fitch et al. (2012) express the momentum tendency in each grid cell as:

$$\frac{\partial |\boldsymbol{V}|_{ijk}}{\partial t} = \frac{\frac{1}{2} N_t^{ij} C_T \left(|\boldsymbol{V}|_{ijk} \right) \boldsymbol{V}_{ijk}^2 A_{ijk}}{(z_{k+1} - z_k)} \tag{1}$$

where A_{ijk} is the cross-sectional rotor area of one wind turbine, N_{ij} is the number of wind turbines per square meter, C_T is the turbine thrust coefficient (the total fraction of KE extracted from the atmosphere due to wind turbines), and z_k is the height of the model at level k. The amount of TKE produced in each grid cell by turbines is expressed as:

$$\frac{\partial TKE_{ijk}}{\partial t} = \frac{\frac{1}{2} N_t^{ij} C_{TKE} \left(|\boldsymbol{V}|_{ijk} \right) \boldsymbol{V}_{ijk}^3 A_{ijk}}{(z_{k+1} - z_k)} \tag{2}$$

where C_{TKE}=C_T-C_P (C_P is the fraction of KE converted into electricity by the wind turbines). Finally, the amount power generated in each grid cell is given by:

$$\frac{\partial P_{ijk}}{\partial t} = \frac{\frac{1}{2} N_t^{ij} C_p \left(|\boldsymbol{V}|_{ijk} \right) \boldsymbol{V}_{ijk}^3 A_{ijk}}{(z_{k+1} - z_k)} \tag{3}$$

The wind turbines perturb the turbulent fluxes within the boundary layer both at, and downstream of the wind farm array. As time proceeds in the model, the planetery boundary layer (PBL) scheme tries to mix away the turbulent fluxes as they are advected.

This study uses a new wind farm parameterization for the WRF model (Fitch et al. (2012)) to assess the impact of the proposed offshore Cape Mendocino wind farm array on the surrounding atmosphere, and to assess whether the calculation by Dvorak et al. (2010) is an over estimate of the average wind power production. We model 352 5 MW REpower offshore wind turbines over an area of 361 km^2 to re-create the farm proposed by Dvorak et al. (2010). Since the turbines in this study are spaced at roughly a 9-rotor by 9-rotor diameter distance (versus a 4-rotor by 7-rotor diameter distance in Dvorak et al.), estimates given of power production loss due to turbine wake may be conservative.

3. Model configuration

The Advanced Research WRF (ARW; v3.4; Skamarock et al. (2008)) is used in this study to evaluate the effects of wind turbine wake in a large offshore wind farm array. The ARW is an Euler nonhydrostatic, fully compressible mesoscale numerical weather prediction model that uses a terrain following hydrostatic pressure coordinate. A 3-day simulation was performed to re-create conditions for the time period of July 9^{th}, 2006. The previous two days were used as model spin-up time. This day was chosen because observed offshore hourly surface wind speeds were high, in

excess of 12 m s^{-1}. Additionally, July has been found to be the windiest month at the Cape Mendocino study site (Dvorak et al. 2010). Two experiments were performed to assess the effects of a wind farm on the atmosphere: (1) with a wind farm parameterized (CTRL) and (2) with no wind farm (NF). Because of the high winds during the period selected, results in this study may yield an upper estimate of the effects of wake on a large turbine array.

The model is ran with four nested domains approximately centered on the proposed Cape Mendocino wind farm location(fig. 1). Two-way feedbacks are enabled between domains to capture wake effects that may persist beyond the innermost domain. The horizontal resolution of each ARW domain was 30-, 10-, 3.33-, and 1.11 km^2, respectively. In the vertical direction there were 30 layers modeled in each domain (top level set to 100 hPa). The timestep for each domain was at 180, 60, 20, and 6.66s, respectively. Time integration was performed by a third order Runga-Kutta solver. Within the model code, the horizontal wind components(u- and v-) were vertically interpolated "on-line" so that they can be output at 100 m (turbine hub height) during run time. This addition to the model may provide better estimates of wind speeds aloft relative to those calculated by extrapolating the surface wind speeds to turbine hub height using a simple power law relation (Peterson and Hennessey 1978).

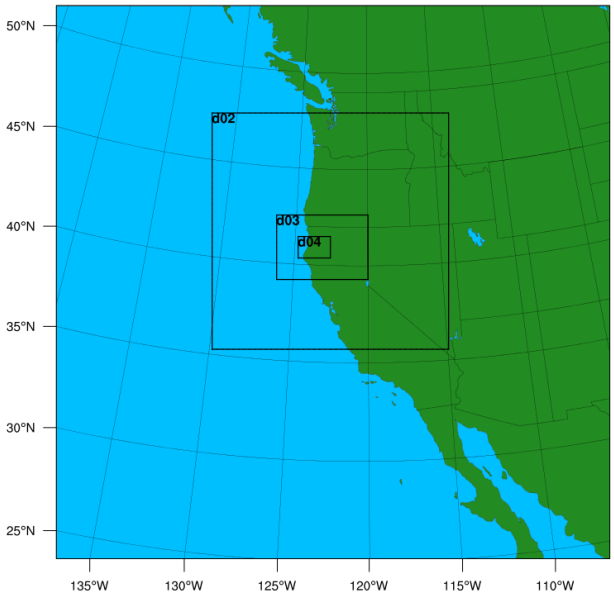

FIG. 2. The ARW domain configuration for the Cape Mendocino wind farm parameterization study.

The model simulation was initialized with the North American Regional Reanalysis (NARR) dataset (Mesinger et al. 2006). The NARR is based on the NCEP Eta model products, with observations integrated using the 3D-Var Data Assimilation System (EDAS). It has a horizontal resolution of 32 km × 32 km and 45 vertical layers with corrections for stability and terrain applied to the extrapolation of winds from the lowest vertical layer to 10 m (Pryor et al. 2009; Pryor and Barthelmie 2010). The NARR are available every 3-hours. Through enhancements in the land surface physics and tropospheric circulation, the NARR data have shown significant improvement over the NCEP2 in surface wind speed biases and fits to rawinsonde observations (Mesinger et al. 2006).

TABLE 1. Table listing the wind turbine parameters for the Fitch et al. (2012) wind turbine ARW parameterization

Turbine hub height	100 m
Rotor diameter	126 m
Standard thrust coefficient	0.158
Cut-in speed	3.500 m s^{-1}
Cut-out speed	30.000 m s^{-1}
Maximum power generation	5.075 MW
Wind turbines per grid cell	1
x-extent of wind farm	17
y-extent of wind farm	17
x-coordinate of SW corner	32
y-coordinate of SW corner	38

The Fitch et al. (2012) wind turbine parameterizations require that the WRF planetary boundary layer (PBL) physics use the Mellor-Yamada-Nakanishi-Niino (MYNN) 2.5 level model(Nakanishi and Niino 2009). The MYNN scheme was selected by (Fitch et al. 2012) because of its known ability to well predict TKE, an important variable that is coupled to the wind farm parameterization. The MYNN surface layer physics were also selected. The RRTM longwave and Goddard shortwave radiation physics options were used. The land-surface model used was the unified Noah land-surface scheme.

The Fitch et al. scheme is initialized in the physics block of the ARW namelist.input file and the turbines modeled are 5 MW REpower offshore wind turbines. One wind turbine is placed in each 1.11 km × 1.11 km grid cell within the wind farm boundary. Typical spacing for offshore wind turbines is 8 rotor diameters (Fitch et al. 2012). The specific wind turbine parameters used in this experiment are given in table 1.

4. Model surface wind speed evaluation

The modeled surface wind speeds on July 9^{th}, 2006 were evaluated for their ability to re-create observed conditions at two locations within the innermost modeled domain for the no farm (NF) simulation. Admittedly, a better assessment of model performance would be to use a longer obser-

vation record to evaluate a longer model simulation, however computational resources for this more comprehensive evaluation exercise were not available at the time of this study, therefore only 1-day of modeled hourly wind speeds are evaluated. It is hypothesized that accurately produced surface wind speeds will bring confidence to the wind speed estimates at turbine hub height (100 m). The only source of un-extrapolated, measured wind speed data aloft is from rawinsonde and radiosonde soundings, which are typically limited to two launches per day. Wind speed observations over land were from the Arcata/Eureka Regional Airport. The wind speeds at the airport were measured at a height of 10 m and are not extrapolated. The airport lies less than 1 km from the Pacific Ocean. Observed wind speeds over water were measured at the National Oceanic and Atmospheric Administration (NOAA) buoy 46022 which lies 17 nautical miles (nm) WSW of Eureka, CA. The wind speeds at the buoy are measured at 5 m, but were extrapolated to 10 m using a power law relationship before being placed on the National Climatic Data Center (NCDC) online archives.

Hourly 10 m wind speeds from the grid cell corresponding to the latitude and longitude of both the buoy and the airport anemometer were extracted and compared to the observed measurements. The comparisons at both sites are shown in fig. 3. The ARW model simulation underpredicts (mb=–2.2 m s^{-1}) average 10 m wind speeds at the location of the ocean buoy. The under prediction may stem from the fact that a simple power law relation was used to extrapolate the winds to a 10 m height or from the intrinsically un-ridgid ocean surface. Moreover, the model simulation is initialized by the NARR which has shown poor performance in reproducing observed surface wind speeds over California (Rasmussen et al. 2011). Nonetheless, the model well captures the diurnal variability of the wind speed at the buoy (r^2=0.68).

At the location of the Arcata/Eureka Regional Airport, the ARW model over predicts the slowest hourly 10 m wind speeds by over 1 m s^{-1}. The ARW has shown poor performance in a previous study when simulating low wind speeds (Hu et al. 2010). Overall, the modeled wind speeds are slightly over predicted (mb=+0.8 m s^{-1}) at the airport, but like NOAA buoy 46022, the diurnal variability is well reproduced (r^2=0.70).

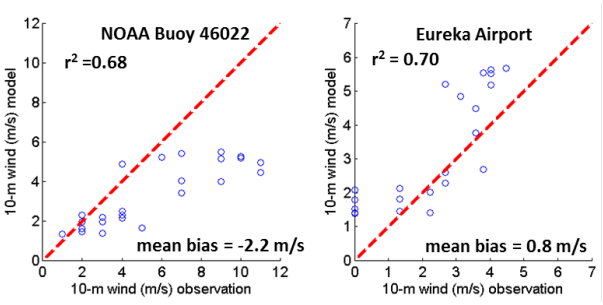

FIG. 3. Scatter plots showing observed 10 m hourly wind speeds (x-axis) versus modeled 10 m hourly wind speeds (y-axis) for July 9^{th}, 2006. The left panel is for NOAA buoy 46022 (17 nm WSW of Eureka, CA); the right panel is for the Arcata/ Eureka Regional Airport. The dashed red line is the 1:1 line.

5. Results and Discussion

a. Effects on modeled wind speeds

The model calculates up to a 3 m s^{-1} reduction in hourly average 100 m wind speeds between the CTRL (wind farm) and NF (no wind farm) scenario for July 9^{th}, 2006 (fig. reffield). Christiansen and Hasager (2005) observed an average reduction in 10 m wind speed of 0.5–1.5 m s^{-1} immediately downstream of the Horns Rev (80 turbines) and the Nysted (78 turbines) offshore wind farms in Denmark while Smalikho et al. (in press) found a reduction in observed wind speeds of 27% to 74% due to wake from one turbine. The reduction in modeled wind speeds due to the turbines in this study extends several kilometers downstream of the wind farm into the third domain (not shown), and Fitch et al. (2012) observed modeled wake effects extending 60 km beyond a modeled offshore wind farm with 100 turbines and a 16% reduction in wind speeds within the wind farm. Christiansen and Hasager (2005) found wind speed deficits 5–20 km downstream of two offshore wind farms while Smalikho et al. (in press) observed wake extending from 120 m up to 1180 m downwind of one turbine.

Modeled wind speeds are reduced (0.5–1.5 m s^{-1}) a few kilometers (5–10 km) upstream of the farm, a feature also seen in the Fitch et al. (2012) modeling study. Some localized areas along the edge of the turbine wake experience an increase in wind speeds between 0.5–1.5 m s^{-1}.

Although wind speed reductions are modest relative to the overall mean flow, power production is sensitive to such changes as it is a function of velocity cubed (Rasmussen et al. 2011).

A vertical cross section taken through roughly –124.5^{o}E longitude (fig. 5) reveals the impact of the modeled wind turbines on the wind speeds through out the PBL. The greatest reduction in wind speeds are located at the height of the turbine rotors (100 m) and are between 2 and 3 m s^{-1}. Wind speeds decrease above the wind farm by 0.5 m s^{-1} up to a height of nearly 800 m. In a modeled neutral boundary layer, Fitch et al. (2012) observe a 0.1 m s^{-1} reduction in modeled wind speeds up to a height of 700 m. Fitch et al. (2012) found their modeled reductions in wind speed to be insensitive ($<$ 0.1 m s^{-1}) to chosen horizontal (between 1- and 2-km simulations) and vertical resolution

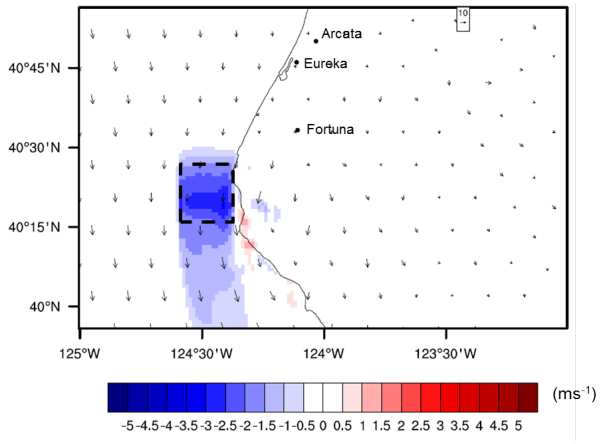

FIG. 4. The change in the 100 m wind speeds (m s^{-1}) between the control and the no wind farm simulations. Wind vectors are from the no farm scenario and the reference vector (upper right hand corner) corresponds to a wind speed of 10 m s^{-1} at a height of 100 m. The black dashed line outlines the location of the parameterized Cape Mendocino wind farm.

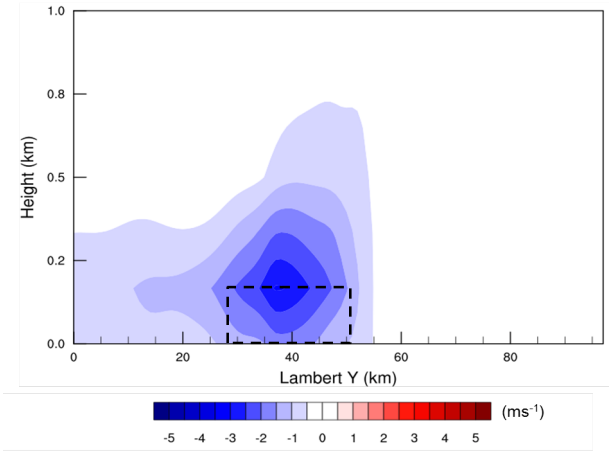

FIG. 5. Vertical cross section of the mean change in the hourly wind speeds (m s^{-1}) over the wind farm between the control and the no farm simulation for conditions on July 9^{th}, 2006. South is the left end of the x-axis while north is the right end of the x-axis. The vertical cross section was taken roughly at –124.5°E longitude and extended from 40°N to nearly 41°N latitude (see fig. 4). Wind speeds are interpolated to height (z) coordinates. The dashed black rectangular box indicates the location of the wind farm.

(81- versus 40-model levels).

b. Effects on power production

Perhaps the most important implication of wind turbine wake is the impact on power production within a large turbine array. Within a 10 × 10 offshore turbine array of 5MW REpower wind turbines, Fitch et al. (2012) find a 40% reduction in modeled power production due to turbine wake effects. Figure 6 shows the change in power potential in the wind due to the wind turbine parameterizations that simulate wake effects for this study. The change is calculated as the relative difference in the cube of the wind speed between the CTRL and NF scenario. Up to a 40% reduction in power production is seen within the wind farm due to the modeled parameterizations.

Fitch et al. (2012) note that the response of the atmosphere to the modeled wind turbines will be dependent upon wind speed. As mentioned previously (section 3.), this study chose to represent the atmosphere's response to optimal wind resource conditions, therefore the results presented here are likely upper estimates of the effects of wind turbine wake on wind power production at the Cape Mendocino location.

The NF scenario under predicted observed wind speeds by 2.2 m s^{-1} at an offshore buoy 17 nm SW of Eureka, CA and over predicted observed wind speeds by 0.8 m s^{-1} at the Arcata/ Eureka Regional Airport. These wind speed biases are within the range of the changes predicted by the Fitch et al. (2012) parameterizations. Moreover, the power function is dependent upon the cube of the wind speed, and small wind speed biases can be amplified if considering power production. Despite the poor performance of the NF scenario in recreating observed wind speeds, the modeled wake effects are of similar magnitude to those in previous observation-based studies (Christiansen and Hasager 2005; Smalikho et al. in press). The findings in this study suggest that the average power production potential for the proposed Cape Mendocino wind farm may be less than the 790 MW calculated by Dvorak et al. (2010). However, more model evaluation is needed before the quantitative wake effects presented in this study can be considered statistically significant.

6. Conclusion

This study used the Fitch et al. (2012) wind turbine parameterizations for a numerical weather prediction model (WRF) to calculate the impact of turbine wake effects on a proposed large offshore turbine array at Cape Mendocino. Dvorak et al. (2010) calculate that an offshore wind farm at Cape Mendocino with 300 5 MW REpower turbines could generate roughly 790 MW of electricity on average. This study hypothesizes that this estimate may be overstated due to neglecting the effects of turbine wake. Two 3-day numerical modeling simulations are performed using WRF: (1) with wind turbine parameterizations that treat

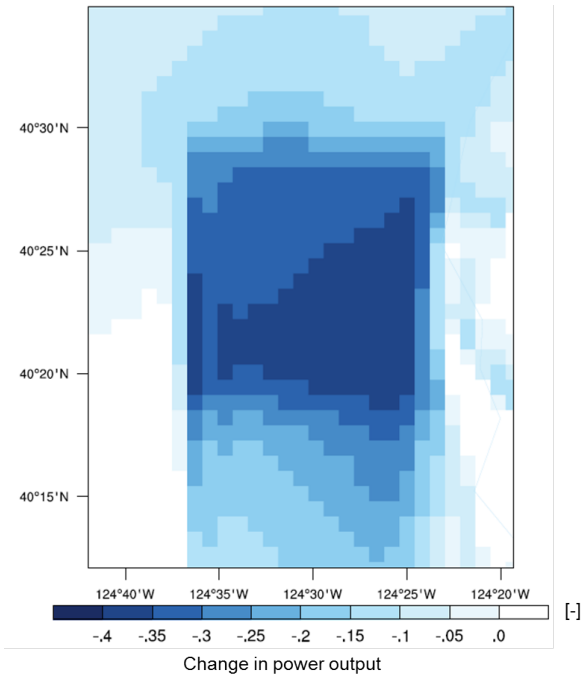

FIG. 6. Change in power potential in the wind due to the Fitch et al. (2012) wind turbine parameterizations that simulate turbine wake effects.

wind turbines as a sink for momentum and as a source of turbulent kinetic energy (TKE) and (2) with no wind turbine parameterization. The simulation with no wind turbines under predicted observed wind speeds by 2.2 m s^{-1} at an offshore buoy 17 nm SW of Eureka, CA and over predicted observed wind speeds by 0.8 m s^{-1} at the Arcata/ Eureka Regional Airport. Results show a decrease in hub-height (100 m) wind speeds of up to 3 m s^{-1} and a 40% reduction in power production within the proposed Cape Mendocino large offshore wind turbine array when using the wind turbine parameterizations. Wind speeds additionally decrease over the wind farm up to a height of 800 m. Despite the model's inability to reproduce observed conditions, the turbine drag effects on wind speed and power production match those from previous observational studies (Christiansen and Hasager 2005; Smalikho et al. in press). The power production potential of the Cape Mendocino wind farm calculated by Dvorak et al. (2010) may be an over estimate because wake effects are neglected. However, more model evaluation is needed before a quantitative estimate of the over prediction can be given with confidence.

Acknowledgments.

The author would like to acknowledge Prof. Shu-Hua Chen (UC-Davis) for help with the addition of the "pmout" code to the WRF model for extracting winds at the turbine hub heights. NARR data provided by the NOAA/OAR/ESRL PSD, Boulder, Colorado, USA, from their Web site at `http://www.esrl.noaa.gov/psd/`. Historical observed wind speed data was obtained from the National Climatic Data Center, Asheville, North Carolina, USA, from their web site at `http://www.ncdc.noaa.gov/oa/ncdc.html`.

REFERENCES

Adams, A. S. and D. W. Keith, 2013: Are global wind power resource estimates overstated? *Environmental Research Letters*, **8 (1)**, 015 021.

Archer, C. L. and M. Z. Jacobson, 2005: Evaluation of global wind power. *Journal of Geophysical Research: Atmospheres*, **110 (D12)**, doi:10.1029/2004JD005462.

Barrie, D. B. and D. B. Kirk-Davidoff, 2010: Weather response to a large wind turbine array. *Atmospheric Chemistry and Physics*, **10 (2)**, 769–775, doi:10.5194/acp-10-769-2010.

CA Senate Bill X1-2, 2011: California's renewable portfolio standard. URL `http://www.cpuc.ca.gov/PUC/energy/Renewables/index.htm`.

Christiansen, M. B. and C. B. Hasager, 2005: Wake effects of large offshore wind farms identified from satellite sar. *Remote Sensing of Environment*, **98 (23)**, 251 – 268, doi:10.1016/j.rse.2005.07.009.

Dvorak, M. J., C. L. Archer, and M. Z. Jacobson, 2010: California offshore wind energy potential. *Renewable Energy*, **35 (6)**, 1244 – 1254, doi:10.1016/j.renene.2009.11.022.

Fitch, A., J. Olson, J. Lundquist, J. Dudhia, A. Gupta, J. Michalakes, and I. Barstad, 2012: Local and mesoscale impacts of wind farms as parameterized in a mesoscale nwp model. *Mon. Wea. Rev.*, **140 (9)**, 3017–3038, doi:10.1175/MWR-D-11-00352.1.

Hu, J., Q. Ying, J. Chen, A. Mahmud, Z. Zhao, S.-H. Chen, and M. J. Kleeman, 2010: Particulate air quality model predictions using prognostic vs. diagnostic meteorology in central california. *Atmospheric Environment*, **44 (2)**, 215 – 226, doi:10.1016/j.atmosenv.2009.10.011.

Jacobson, M. Z. and C. L. Archer, 2012: Saturation wind power potential and its implications for wind energy. *Proceedings of the National Academy of Sciences*, doi:10.1073/pnas.1208993109.

Lu, X., M. B. McElroy, and J. Kiviluoma, 2009: Global potential for wind-generated electricity. *Proceedings of the National Academy of Sciences*, doi:10.1073/pnas.0904101106.

Mesinger, F., et al., 2006: North American Regional Reanalysis. *Bulletin of the American Meteorological Society*, **87 (3)**, 343–360, doi:10.1175/bams-87-3-343.

Nakanishi, M. and H. Niino, 2009: Development of an improved turbulence closure model for the atmospheric boundary layer. *Journal of the Meteorological Society of Japan. Ser. II*, **87 (5)**, 895–912.

Peterson, E. W. and J. P. Hennessey, 1978: On the use of power laws for estimates of wind power potential. *J. Appl. Meteor.*, **17 (3)**, 390 – 394, doi:10.1175/1520-0450(1978)017⟨0390:OTUOPL⟩2.0.CO;2.

Pryor, S. and R. Barthelmie, 2010: Climate change impacts on wind energy: A review. *Renewable and Sustainable Energy Reviews*, **14 (1)**, 430 – 437, doi:10.1016/j.rser.2009.07.028.

Pryor, S. C., et al., 2009: Wind speed trends over the contiguous united states. *Journal of Geophysical Research: Atmospheres*, **114 (D14)**, doi:10.1029/2008JD011416.

Rasmussen, D. J., T. Holloway, and G. F. Nemet, 2011: Opportunities and challenges in assessing climate change impacts on wind energya critical comparison of wind speed projections in california. *Environmental Research Letters*, **6 (2)**, 024 008.

Skamarock, W., J. Klemp, J. Dudhia, D. Gill, D. Barker, M. Duda, X. yu Huang, and W. Wang, 2008: A description of the advanced research wrf version 3. Tech. rep., University Corporation for Atmospheric Research. doi:10.5065/D68S4MVH.

Smalikho, I. N., V. A. Banakh, Y. L. Pichugina, W. A. Brewer, R. M. Banta, J. K. Lundquist, and N. D. Kelley, in press: Lidar investigation of atmosphere effect on a wind turbine wake. *J. Atmos. Oceanic Technol.*, doi:10.1175/JTECH-D-12-00108.1.